Dubna-Mainz-Taipei (DMT) dynamical model for pion scattering and EM meson production

Shin Nan Yang
National Taiwan University

Collaborators:
Dubna: Kamalov
Mainz: Drechsel, Tiator
Taipei: GY Chen, CT Hung, CC Lee, SNY

The 10th International Workshop on the Physics of Excited Nucleons
(NSTAR2015) , May 25 – 28 Thu, 2015
Osaka University, Osaka, Japan

Outline

- Motivation
- DMT πN model
- DMT model for electromagnetic production of pion
- Results
  - threshold production
  - resonances properties
- Summary

Motivation

- To construct a meson-exchange model for **πN scattering** and **e.m. production of pion** to achieve a unified description for both reactions over a wide range of energies, i.e., from threshold to ~ 2 GeV.

- comparison with **ChPT** predictions near threshold to gain a glimpse of chiral symmetry

- **consistent extraction** of the resonance properties like, mass, width, and form factors, from both reactions.
  - Comparison with LQCD results requires reliable extraction. **consistent extractions** → minimize model dependence ?

- The resonances studied are always **assumed** to be of the type which results from dressing of the quark core by meson cloud.
  → **understand the underlying structure and dynamics**

History of DMT model

- J. Phys. ***G* 11**, (1985) L205.
  - Dynamical approach for pion photoproduction reaction proposed
- J. Phys ***G* 20**, (1994) 1531; Phys. Rev *C* **64**, (2001) 034309.
  – Taipei-Argonne meson-exchange πN model (in collab w/H.T-S. Lee)
- Phys. Rev. Lett. **83**, (1999) 4494.
  - DMT results for Δ deformation
- Phys. Rev. *C* **64**, (2001) 032201; Phys. Lett. **B 522**, (2001) 27.
  - DMT results for form factors and threshold π production
- Nucl. Phys. ***A* 723**, (2003) 447; Phys. Rev. ***C* 76**, (2007) 035206.
  – DMT results for nucleon higher resonances

http://portal.kph.uni-mainz.de/MAID//dmt/

Taipei-Argonne πN model:

meson-exchange π N model below 400 MeV

Bethe-Salpeter equation

$$T_{\pi N} = B_{\pi N} + B_{\pi N} G_0 T_{\pi N},$$

where

$B_{\pi N} =$ sum of all irreducible two-particle Feynman amplitues

$G_0 =$ relativistic free pion-nucleon propagator

can be rewritten as $\Rightarrow$

$$T_{\pi N} = \overline{B}_{\pi \mathrm{N}} + \overline{B}_{\pi \mathrm{N}} \overline{G}_0 T_{\pi N},$$

with

$$\overline{B}_{\pi \mathrm{N}} = B_{\pi N} + B_{\pi N} (G_0 - \overline{G}_0) \overline{B}_{\pi N}.$$

Three-dimensional reduction

Choose a $\overline{G}_0(k,P)$ such that

1. $T_{\pi N} = \overline{B}_{\pi N} + \overline{B}_{\pi N}\overline{G}_0 T_{\pi N}$ becomes three-dimensional

2. $\overline{G}_0$ can reproduce πN elastic cut

Cooper-Jennings reduction scheme

It satisfies both

the soft pion theorems and unitarity

Cooper, Jennings, NP A483, 601 (1988).

Approximate $\overline{B}_{\pi N}$ by

tree approximation of a **chiral** **effective Lagrangian**

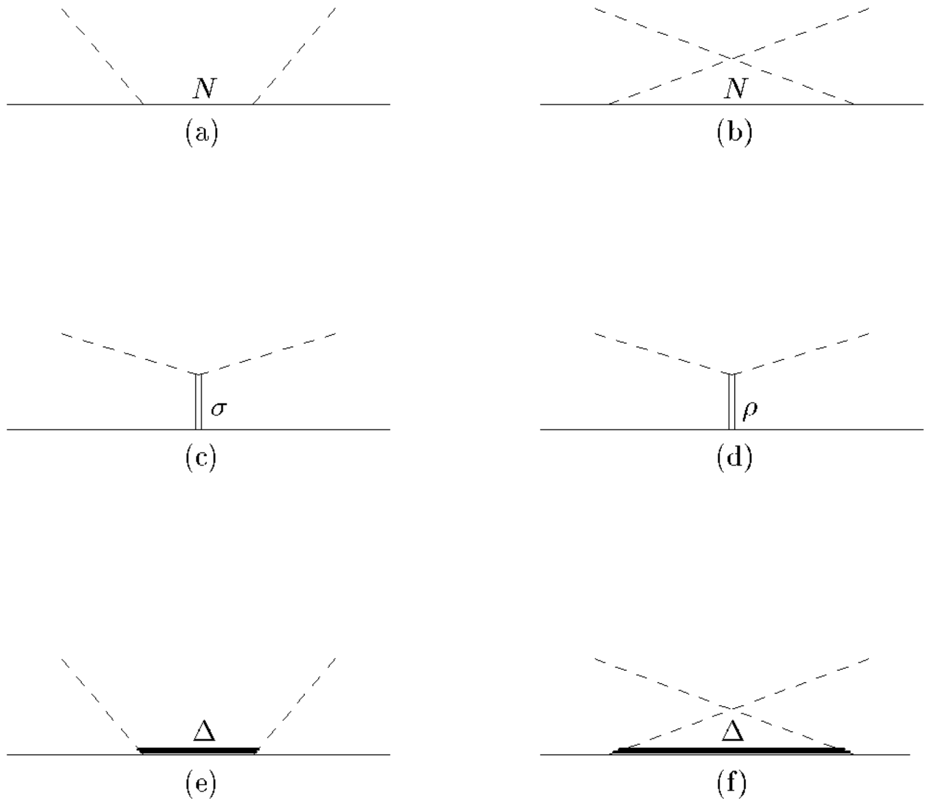

$$F\left(p^2\right)=\left[\frac{n\Lambda^4}{n\Lambda^4+\left(m^2-p^2\right)^2}\right]^n,$$

$$n=10$$

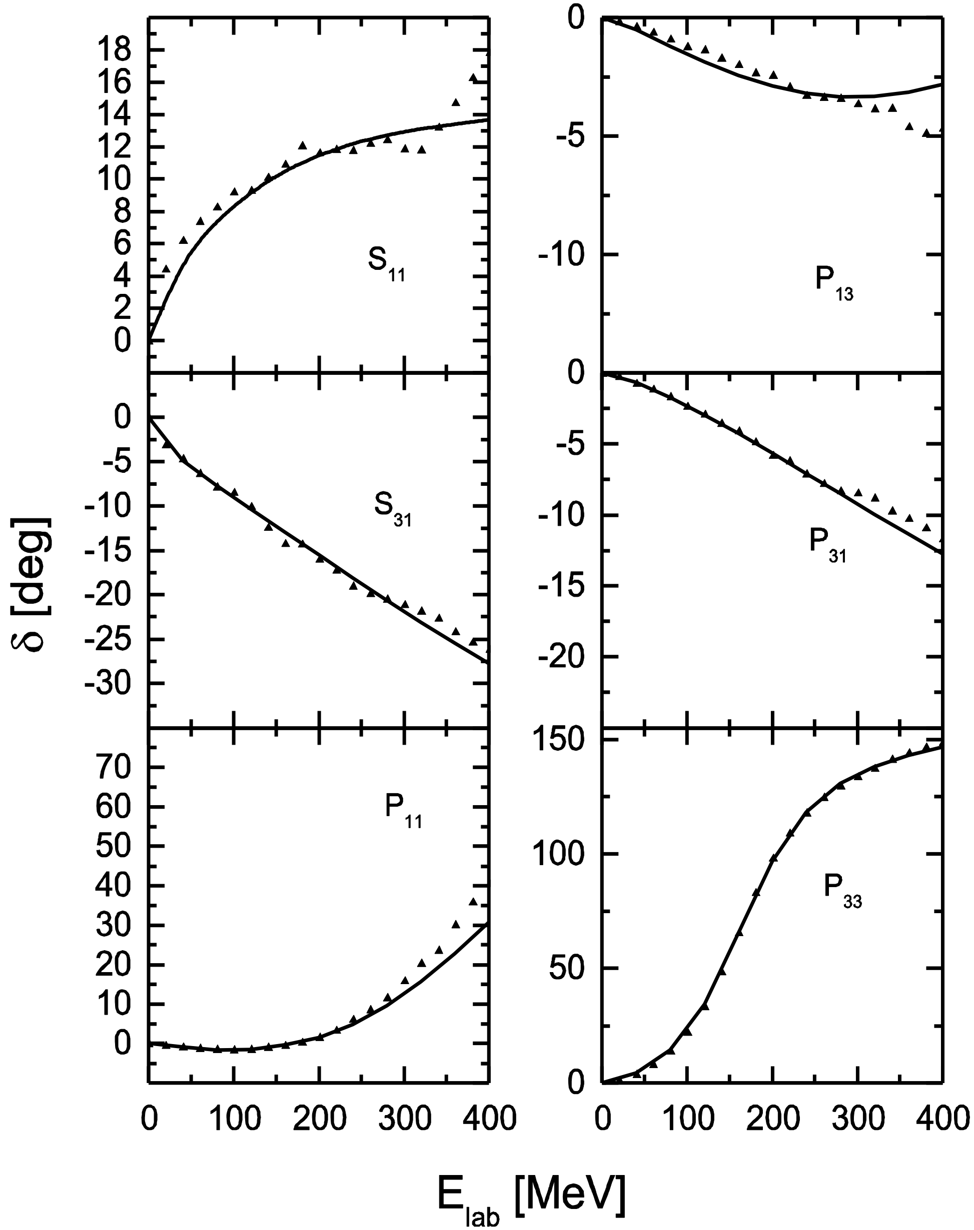

13 parameters

C.T. Hung, S.N. Yang, and T.-S.H. Lee, Phys. Rev. C64, 034309 (2001)

Dynamical model for γ N $\rightarrow$ π N

To order e, the t-matrix for γ N $\rightarrow$ π N is written as

$$t_{\gamma\pi}(E) = v_{\gamma\pi} + v_{\gamma\pi} g_0(E) t_{\pi N}(E),$$

where

$$v_{\gamma\pi} = \text{transition potential},$$

$$t_{\pi N} = \pi N \ t\text{-matrix},$$

two ingredients

$v_{\gamma\pi}$, $t_{\pi N}$

Both on- & off-shell

(gauge invariance?)

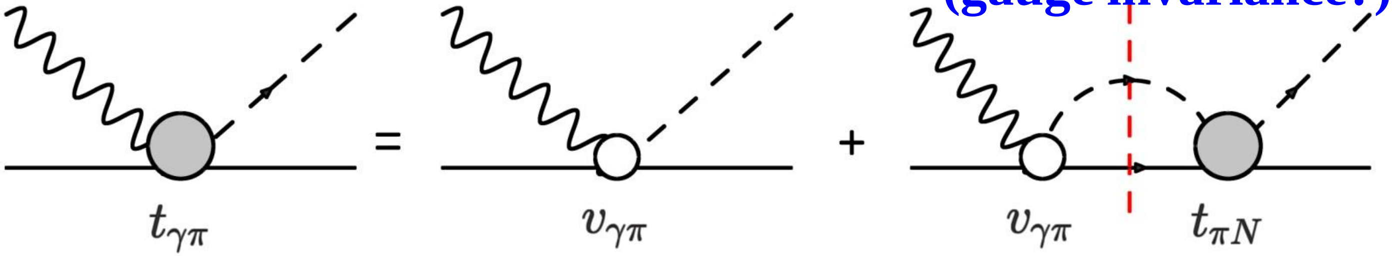

- Multipole decomposition of $t_{\gamma\pi}$ gives the physical amplitude in channel α=(ξ , $l\pi$, j),

$$t_{\gamma\pi}^{(\alpha)}(q_E,k;E+i\varepsilon)=\exp(i\delta^{(\alpha)})\cos\delta^{(\alpha)}$$
$$\times\left[v_{\gamma\pi}^{(\alpha)}(q_E,k)+P\int_0^\infty dq'\frac{q'^2 R_{\pi N}^{(\alpha)}(q_E,q';E)\,v_{\gamma\pi}^{(\alpha)}(q',k)}{E-E_{\pi N}(q')}\right]$$

where

- $\delta^{(\alpha)}$, $R_{\pi N}(\alpha)$: π N scattering phase shift and reaction matrix in channel α
- k=| k|, q_E : photon and pion on-shell momentum

Both on- & off-shell
(gauge invariance?)

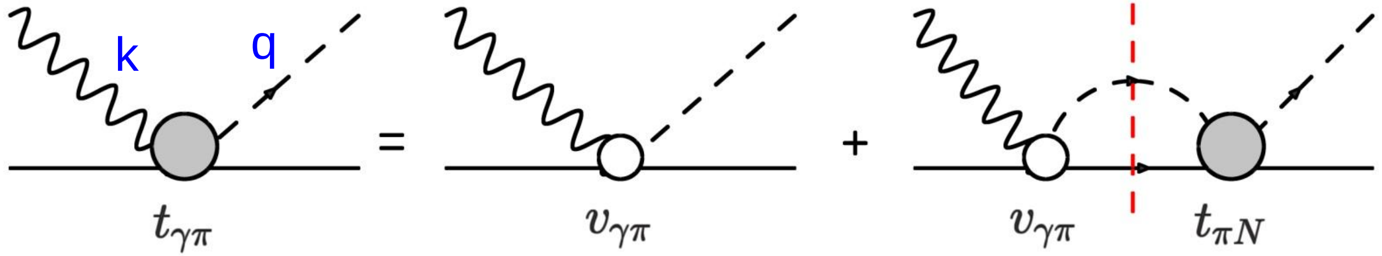

DMT Model $v_{\gamma\pi}^{B}$ obtained from tree diagrams of a chiral effective Lagrangian

$v_{\gamma\pi}^{B} =$

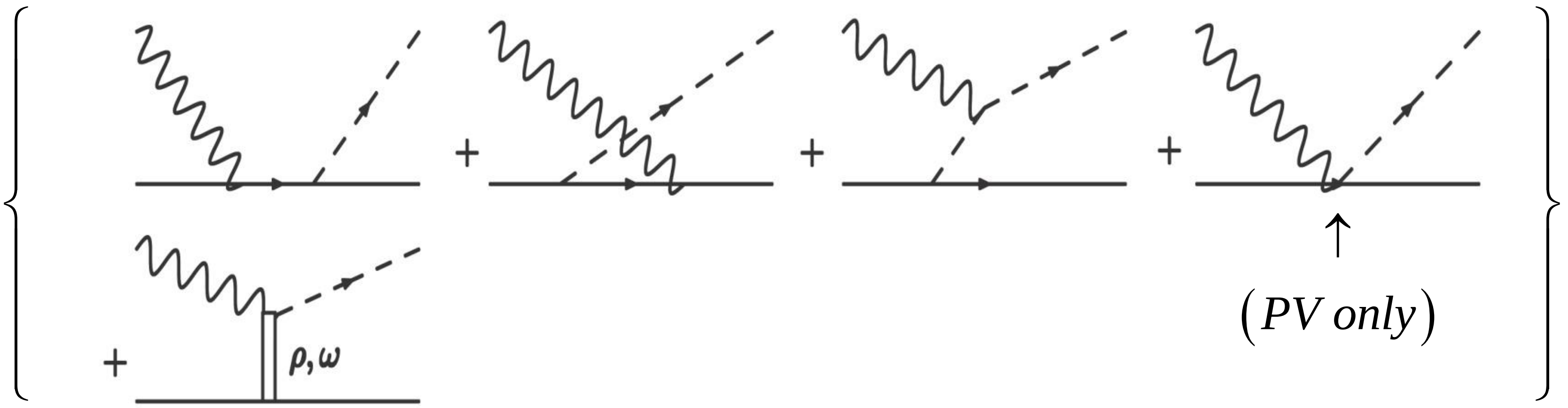

Results of DMT model near threshold

(depends only on $v^B_{\lambda\pi}$ and $t^B_{\pi N}$)

$\vec{\gamma} + p \rightarrow \pi^0 + p$, Σ : E_γ = 145 – 190 MeV

Hornidge et al., PRL 111, (2013) 062004

A2 and CB-TAPS Collab. @ MAMI

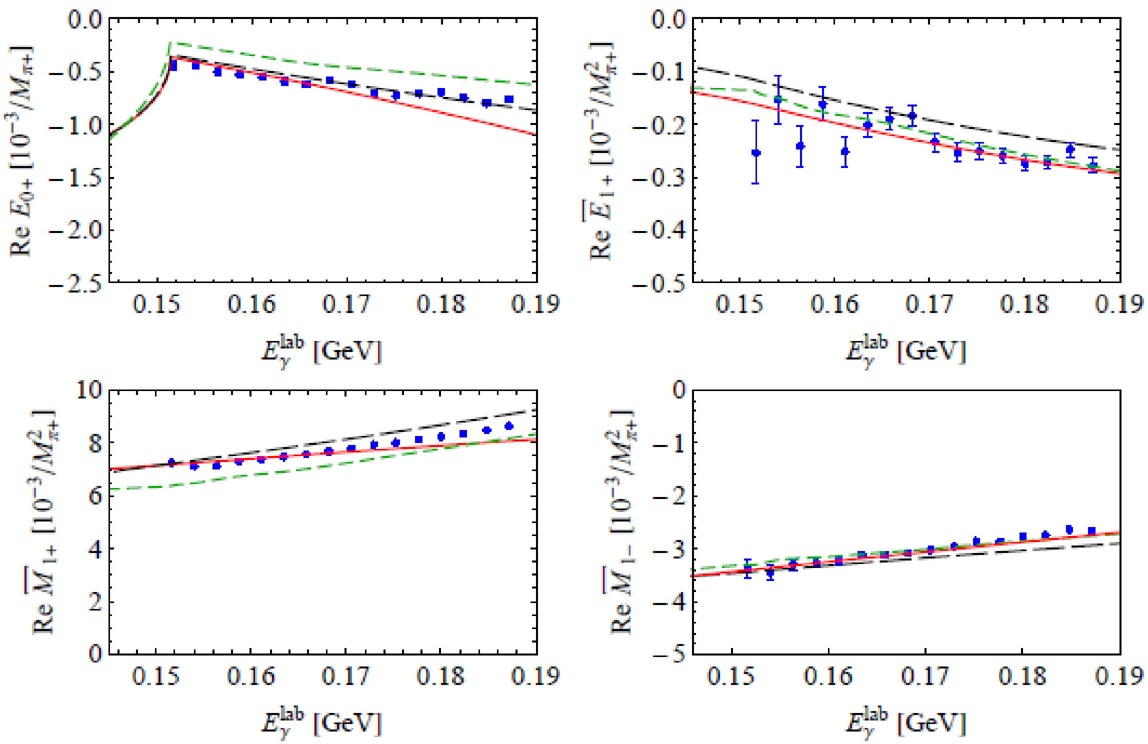

- - - - - : **DMT**

— — — : Gasparyan and Lutz , unitary EFT w/ chiral Lagrangian

——— : RChPT (Hilt, Scherer & Tiator)

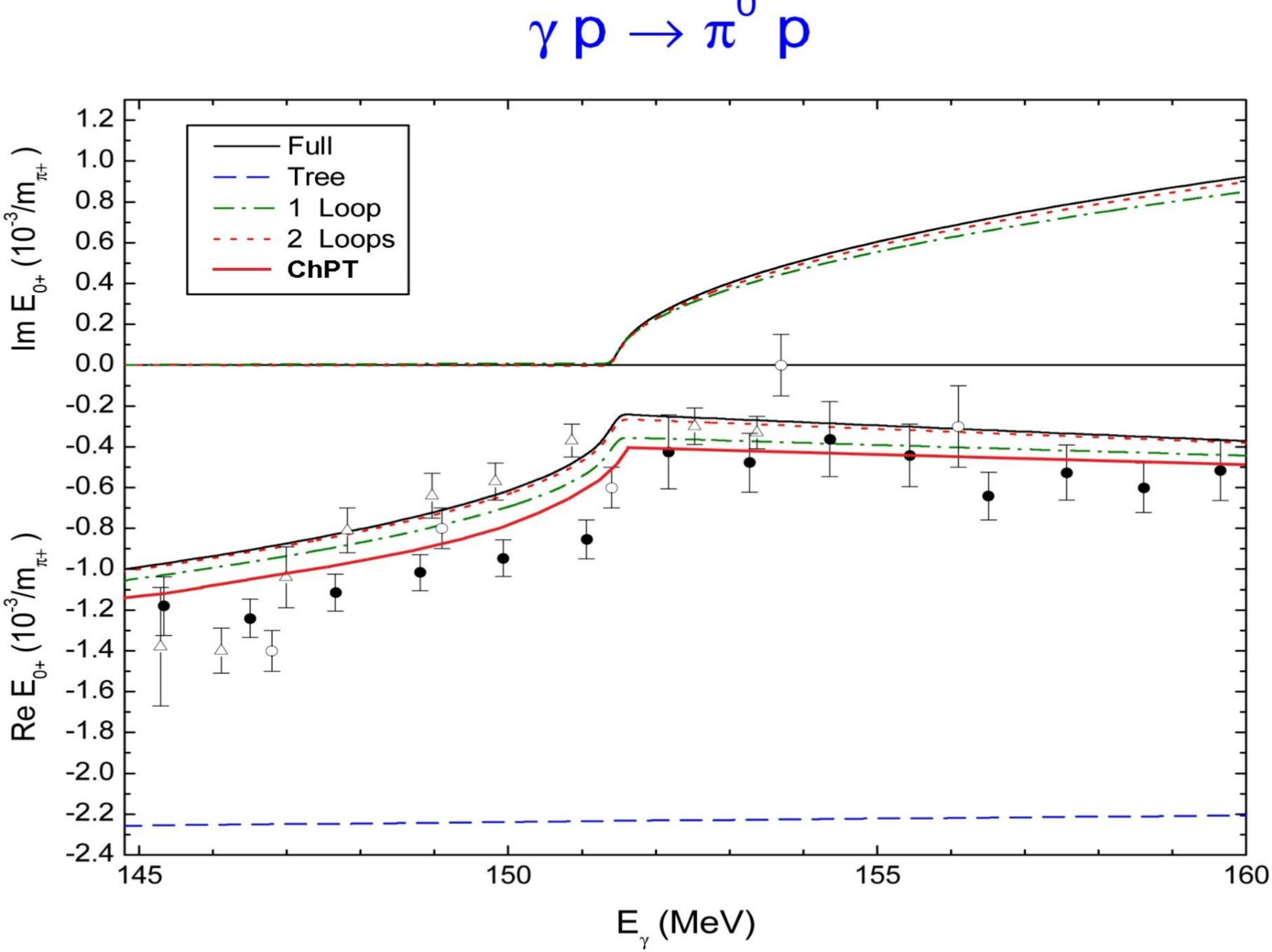

$\gamma\, p \to \pi^0\, p$
Full
Tree
1 Loop
2 Loops
ChPT
Im E_{0+} ($10^{-3}/m_{\pi+}$)
Re E_{0+} ($10^{-3}/m_{\pi+}$)
E_γ (MeV)

$\gamma + \vec{p} \rightarrow \pi^0 + p$, σ_T : E_γ = 145 - 190 MeV

S. Schumann et al., A2 Collab. @ MAMI, submitted to PL B.

$$\sigma_T = \sigma_0 T,$$

$$T = \frac{1}{P_T \sin\varphi} \frac{\sigma_+ - \sigma_-}{\sigma_+ + \sigma_-},$$

P_T : target pol.

φ: π^0 azimuthal angle

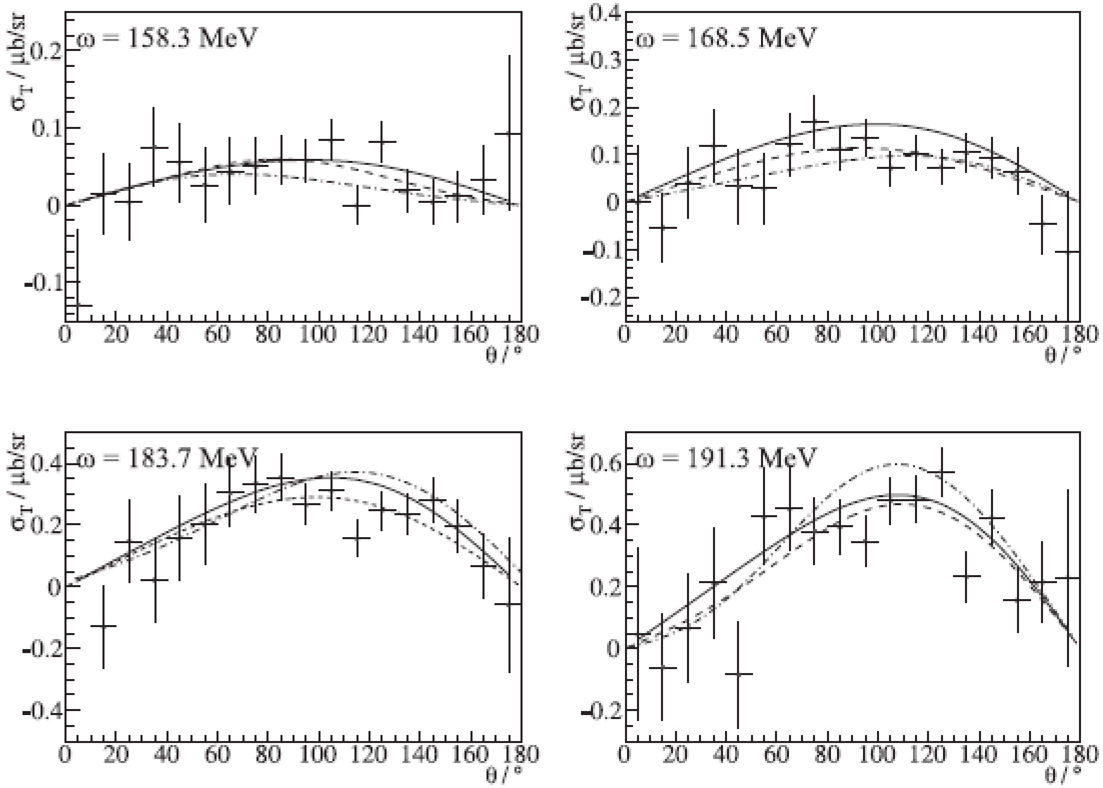

——— : DMT, -·-·-·- , ---------- fits

$$\sigma_T = \frac{q}{k}\sin\theta\left[t_0 P_0(\cos\theta) + t_1 P_1(\cos\theta)\right]$$

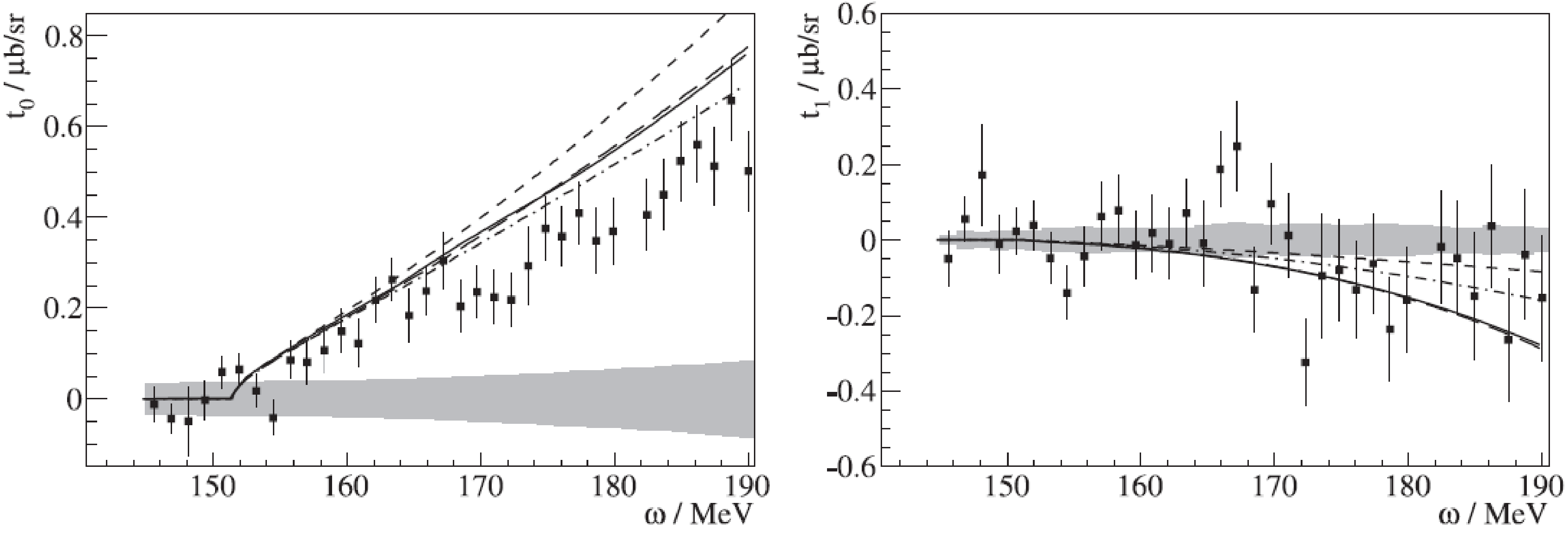

: DMT

: Gasparyan – Lutz

: RChPT

: fit of Hornidge et al.

$$\frac{d\sigma_v}{d\Omega_\pi} = \frac{d\sigma_T}{d\Omega_\pi} + \epsilon\frac{d\sigma_L}{d\Omega_\pi} + \sqrt{2\epsilon(1+\epsilon)}\frac{d\sigma_{LT}}{d\Omega_\pi}\cos\Phi_\pi + \epsilon\frac{d\sigma_{TT}}{d\Omega_\pi}\cos 2\Phi_\pi + h\sqrt{2\epsilon(1-\epsilon)}\frac{d\sigma_{LT'}}{d\Omega_\pi}\sin\Phi_\pi$$

$Q^2 = 0.05$ GeV^2, $\Theta_\pi = 90°$, $\Phi_\pi = 90°$, and $\epsilon = 0.93$

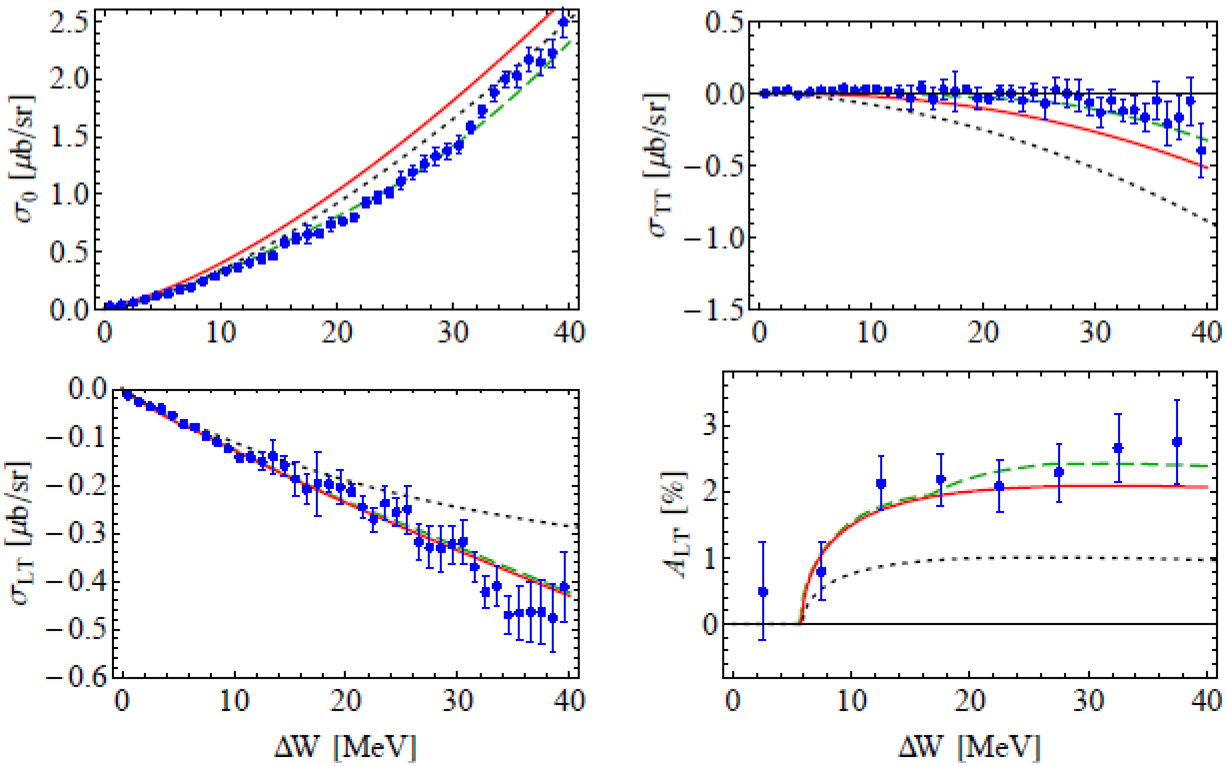

data: M. Weis et al., Eur. Phys. J. A 38 (2008) 27
- - - -: **DMT**
: HBChPT [Bernard et al., PLB 383, 116 (1996)]
: RChPT (Hilt, Scherer & Tiator, 2013)

Chirapatpimol et al., PRL 114, 192503 (2015) , Hall A Collab.
$p(e,e'p)\pi^0$ with E_e = 1192 MeV

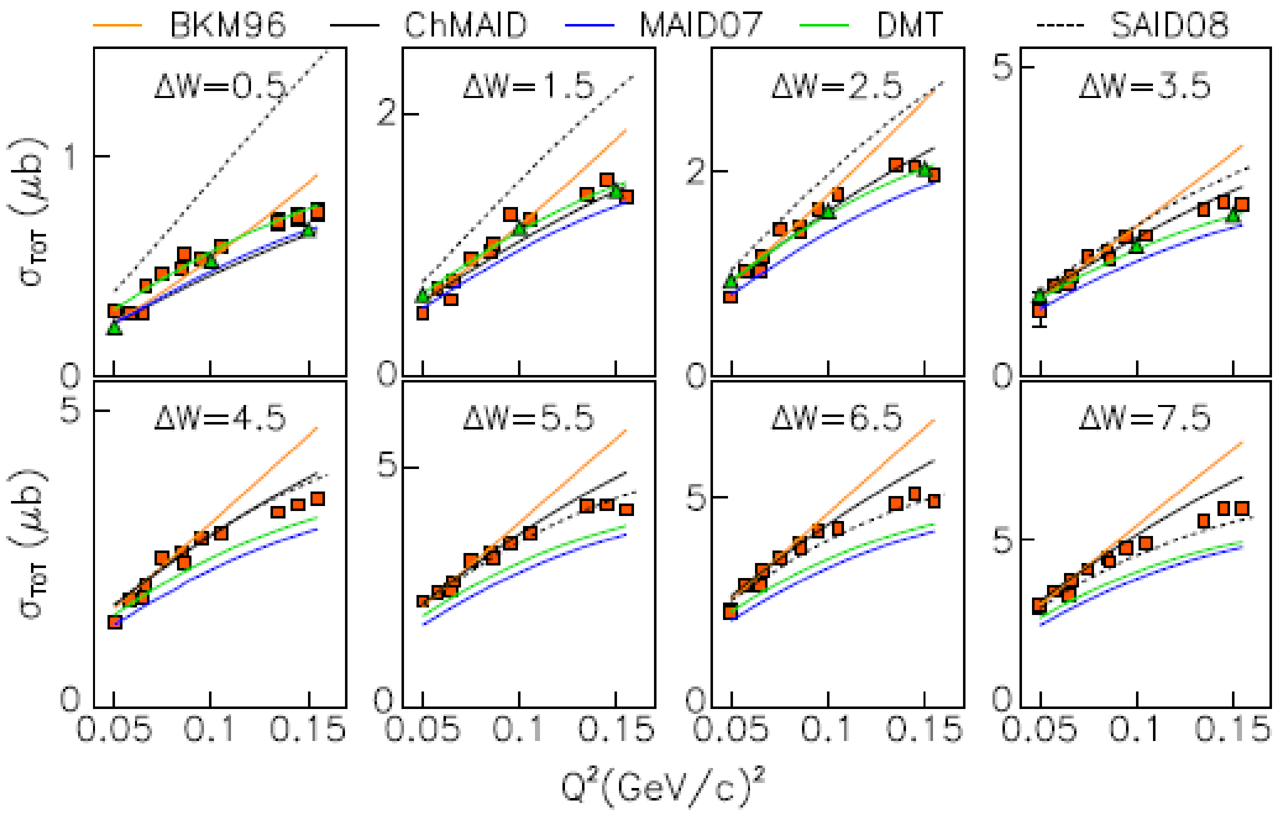

$$\frac{d\sigma}{d\Omega_\pi^*} = \frac{p_\pi^*}{k_\gamma^*}\Big(R_T + \epsilon_L R_L + \epsilon R_{TT}\cos 2\phi_\pi^* + \sqrt{2\epsilon_L(\epsilon+1)}R_{LT}\cos\phi_\pi^*\Big).$$

$$R_T + \epsilon_L R_L = A_0^{T+L} + A_1^{T+L} P_1(x) + A_2^{T+L} P_2(x),$$

$$R_{TT} = A_0^{TT}(1 - x^2),$$

$$R_{LT} = (A_0^{LT} + A_1^{LT} P_1(x))(1 - x^2)^{1/2}.$$

$$A_0^{T+L} = a_0 + b\left|q_\pi^*\right|^2$$

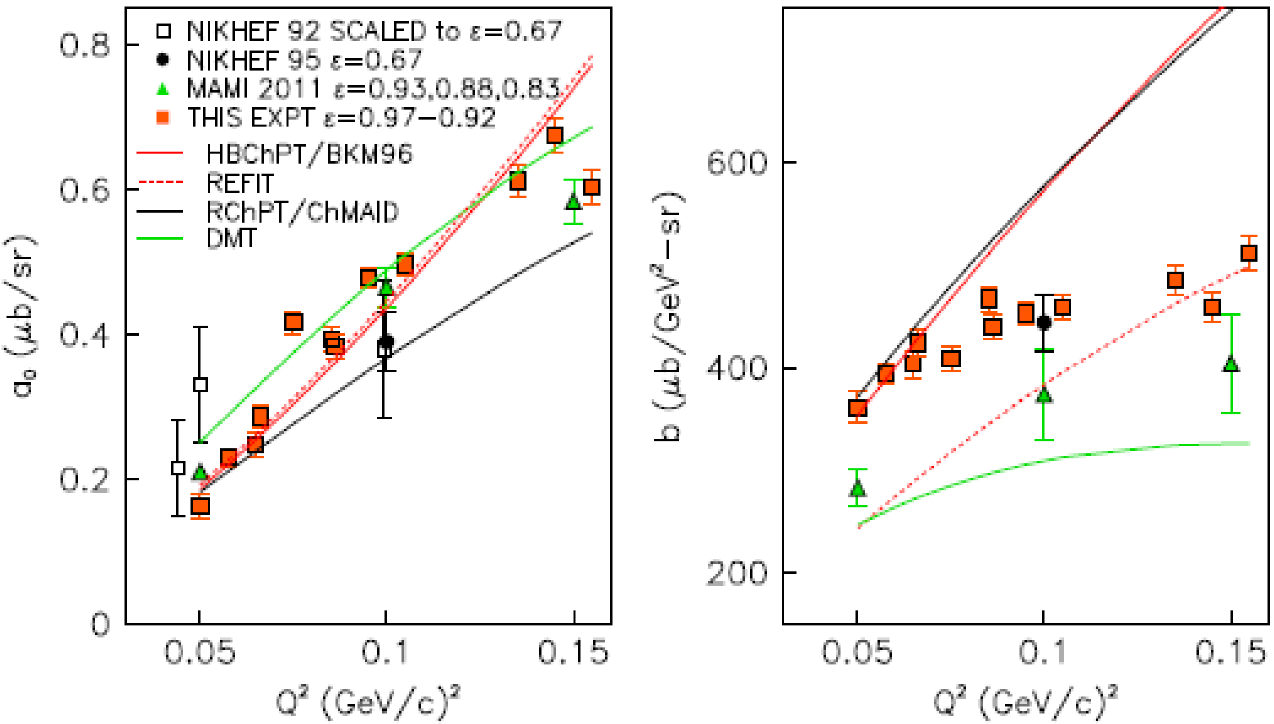

$$R_T + \epsilon_L R_L = A_0^{T+L} + A_1^{T+L} P_1(x) + A_2^{T+L} P_2(x),$$

$$R_{TT} = A_0^{TT}(1 - x^2),$$

$$R_{LT} = (A_0^{LT} + A_1^{LT} P_1(x))(1 - x^2)^{1/2}.$$

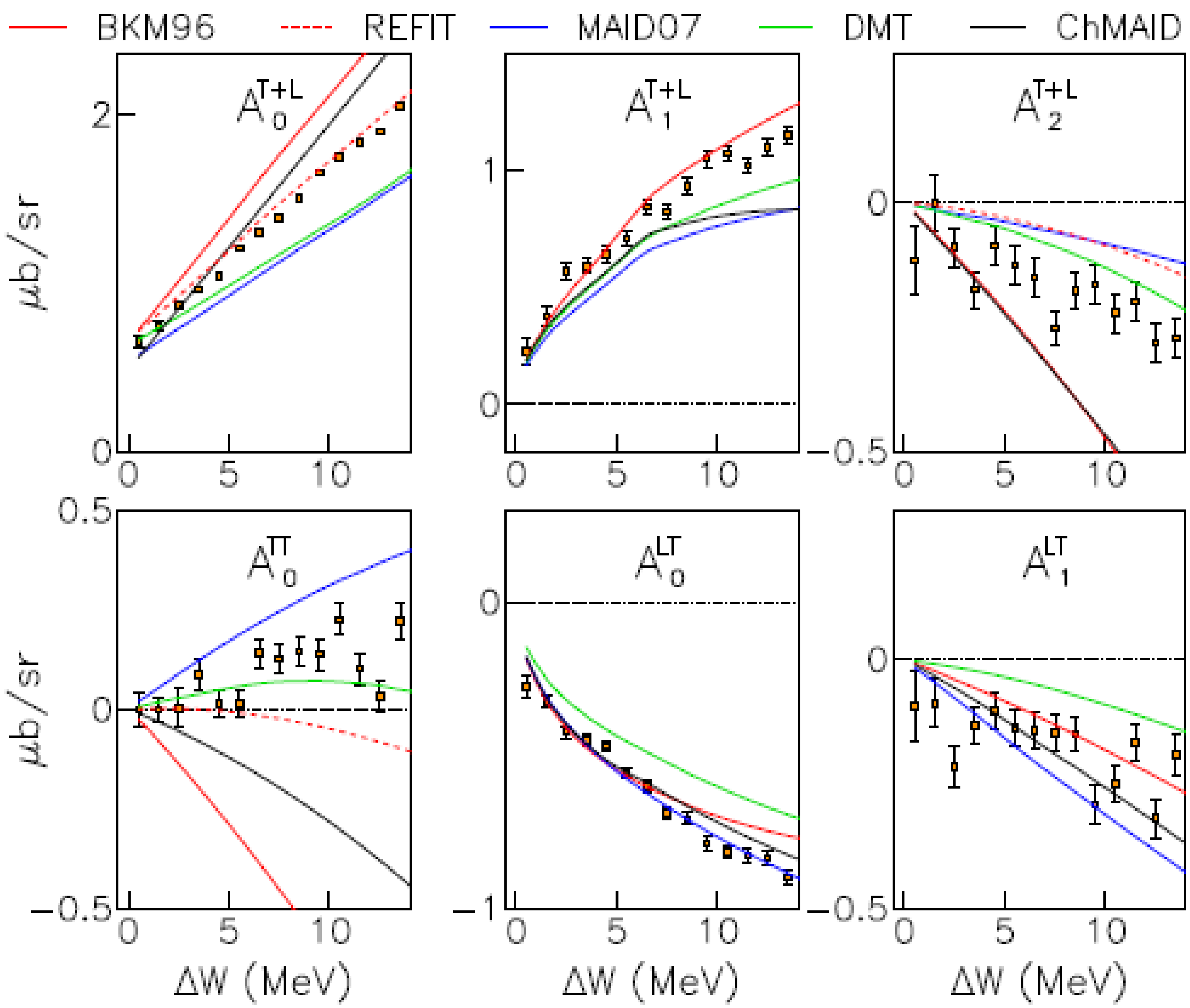

	DMT	HBChPT/ RChPT
chiral symmetry	yes	yes
crossing symmetry	no	yes
unitarity	yes	no
counting	loop	chiral power

If a resonance appears,

then transition potential $v_{\gamma\pi}$ consists ot two terms,

$$v_{\gamma\pi}(E) = v^{B}_{\gamma\pi}(E) + v^{R}_{\gamma\pi}(E),$$

where

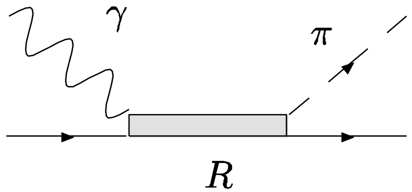

$v^{B}_{\gamma\pi}$ = background transition potential

$v^{R}_{\gamma\pi}$ = contribution of a bare resonance R

then one obtains

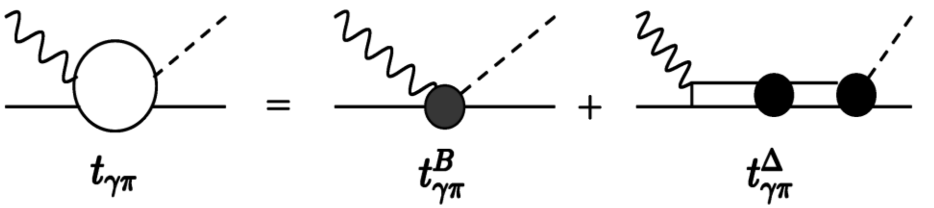

$$t_{\gamma\pi}(E) = t^{B}_{\gamma\pi}(E) + t^{R}_{\gamma\pi}(E),$$

with

$$\begin{cases} t^{B}_{\gamma\pi}(E) = v^{B}_{\gamma\pi} + v^{B}_{\gamma\pi} g_0(E) t_{\pi N}(E) \\ t^{R}_{\gamma\pi}(E) = v^{R}_{\gamma\pi} + v^{R}_{\gamma\pi} g_0(E) t_{\pi N}(E) \end{cases}$$

both t^{B} and t^{R} satisfy Fermi-Watson theorem, respectively.

In DMT, we approximate the resonance contribution $A^R{}_\alpha(W,Q^2)$ by the following Breit-Wigner form

$$A_\alpha^R(W,Q^2) = \bar{A}_\alpha^R(Q^2)\,\frac{f_{\gamma R}(W)\Gamma_R M_R f_{\pi R}(W)}{M_R^2 - W^2 - iM_R\Gamma_R}\,e^{i\phi},$$

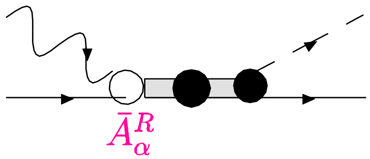

with

$f_{\pi R}$ = Breit-Wigner factor describing the decay of the resonance R

$\Gamma_R(W)$ = total width

M_R = physical mass

$\phi(W)$ = to adjust the phase of the total multipole to be equal to the corresponding π N phase shift $\delta^{(\alpha)}$.

Note that $\bar{A}_\alpha^R(Q^2)$ refers to a bare vertex

- Δ deformation

△ deformation (w/ two parameters GM1 & GE2)
(hyperfine qq interaction → D-state component in the △)

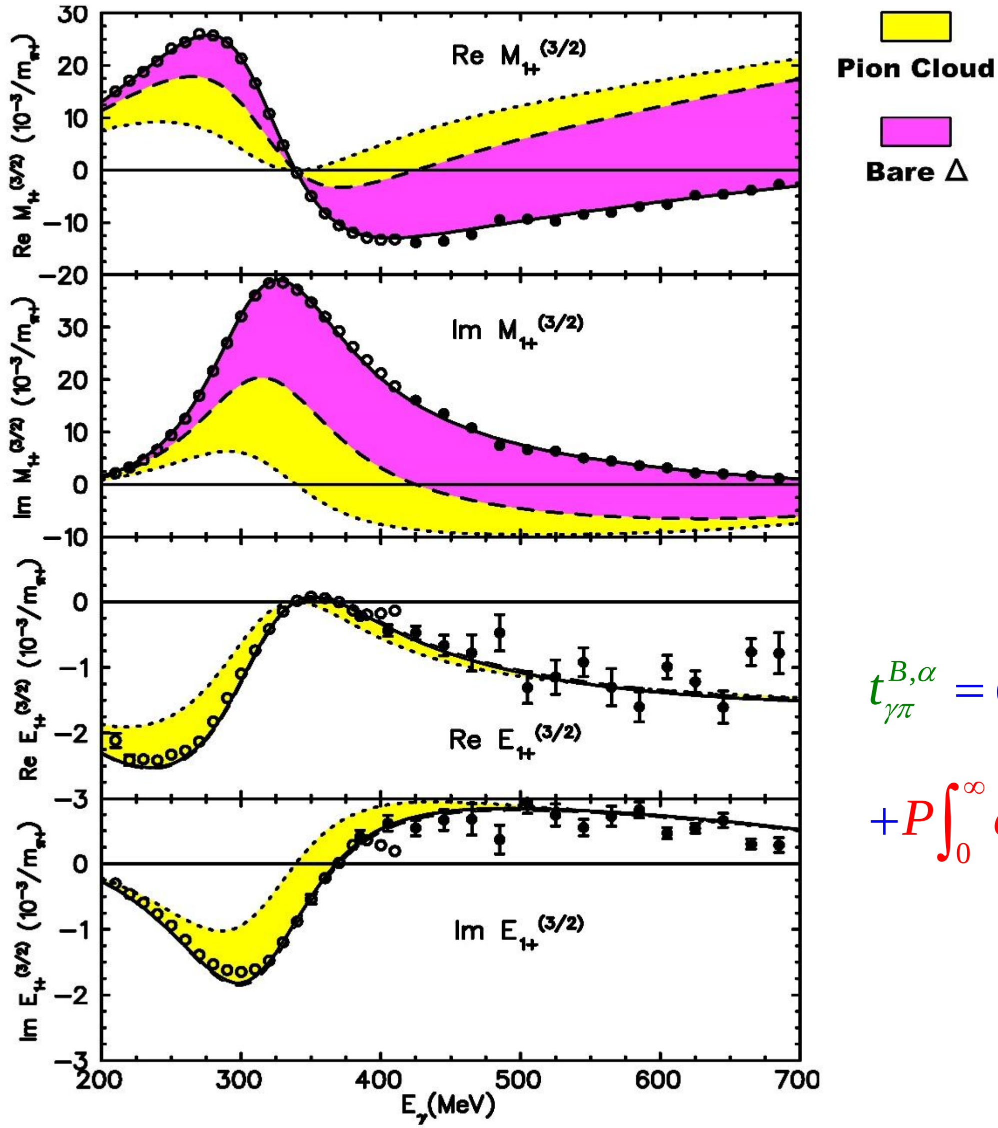

R_{EM} = - 2.4%

Dashed (dotted) curves are results for $t^B_{\gamma\pi}$

including (excluding) the principal value integral contribution.

$$t^{B,\alpha}_{\gamma\pi} = \exp(i\delta^{(\alpha)})\cos\delta^{(\alpha)}\{v^{B,\alpha}_{\gamma\pi}(W,Q^2)$$

$$+P\int_0^\infty dq' \frac{q'^2 R^{(\alpha)}_{\pi N}(q_E,q';E)v^{B,\alpha}_{\gamma\pi}(q',k)}{E-E_{\pi N}(q')}\}$$

	$A_{1/2}$ $(10^{-3} GeV^{-1/2})$	$A_{3/2}$	$Q_{N\to\Delta}$ (fm^2)	$\mu_{N\to\Delta}$
PDG	**-135**	**-255**	**-0.072**	**3.512**
LEGS	**-135**	**-267**	**-0.108**	**3.642**
MAINZ	**-131**	**-251**	**-0.0846**	**3.46**
DMT	**-134** **(-80)**	**-256** **(-136)**	**-0.081** **(0.009)**	**3.516** **(1.922)**
SL	**-121** **(-90)**	**-226** **(-155)**	**-0.051** **(0.001)**	**3.132** **(2.188)**

Comparison of our predictions for the helicity amplitudes, $Q_{N\to\Delta}$ and $\mu_{N\to\Delta}$ with experiments and Sato-Lee's prediction. The numbers within the parenthesis in red correspond to the bare values. Small bare value of $Q_{N\to\Delta}$ indicate that bare Delta is almost spherical.

DMT πN model:

extension of Taipei-Argonne model
to energies $\leq$ 2 GeV

- Inclusion of ηN channel and effects of **$\pi\pi$N channel** in S_{11}
- Introducing higher resonances as indicated by the data

G.Y. Chen et al., Phys. Rev. C 76 (2007) 035206.

decomposition of bkg and reson.

(in the case of only one resonance)

$$t_{\pi N}(E) = t_{\pi N}^{B}(E) + t_{\pi N}^{R}(E),$$

where

$$\begin{cases} t_{\pi N}^{B}(E) = \upsilon_{\pi N}^{B}(E) + \upsilon_{\pi N}^{B} g_0(E) t_{\pi N}(E), \\ t_{\pi N}^{R}(E) = \upsilon_{\pi N}^{R}(E) + \upsilon_{\pi N}^{R} g_0(E) t_{\pi N}(E). \end{cases}$$

Introduction of higher resonances

If there are n resonances, then

$$\upsilon_{ij}^{R}(q,q';E)=\sum_{n=1}^{N}\upsilon_{ij}^{R_n}(q,q';E)$$

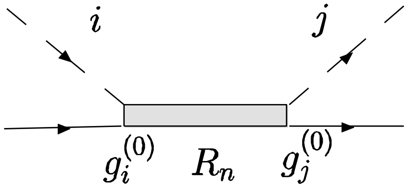

$$\upsilon_{ij}(E)=\upsilon_{ij}^{B}(E)+\upsilon_{ij}^{R}(E)$$

$$t_{ij}(E)=\upsilon_{ij}(E)+\sum_{k}\upsilon_{ik}(E)g_k(E)t_{kj}(E),$$

Coupled-channels equations can be solved

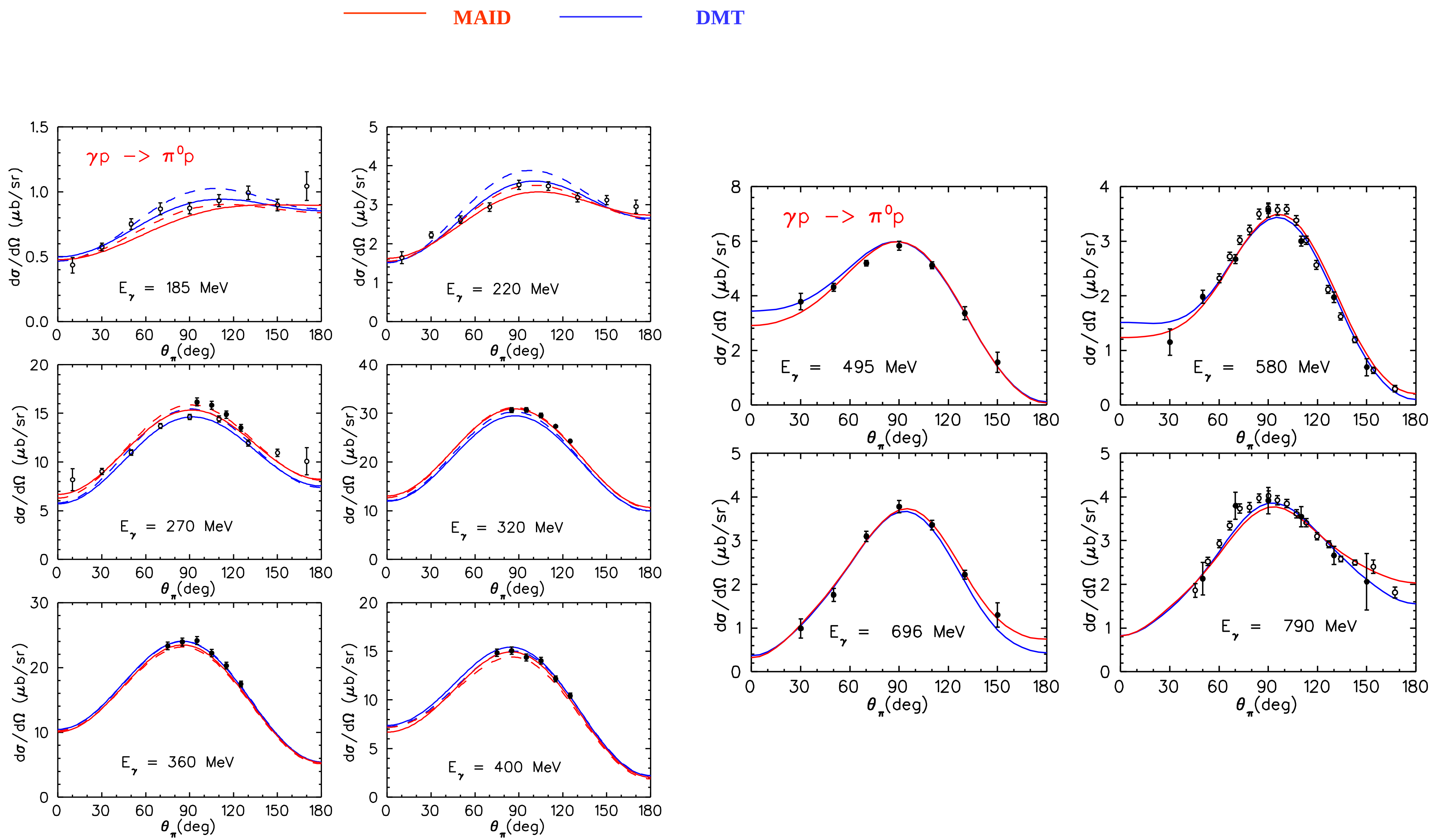

MAID
DMT
γp -> π⁰p
dσ/dΩ (μb/sr)
θ_π(deg)
E_γ = 185 MeV
E_γ = 220 MeV
E_γ = 270 MeV
E_γ = 320 MeV
E_γ = 360 MeV
E_γ = 400 MeV
E_γ = 495 MeV
E_γ = 580 MeV
E_γ = 696 MeV
E_γ = 790 MeV

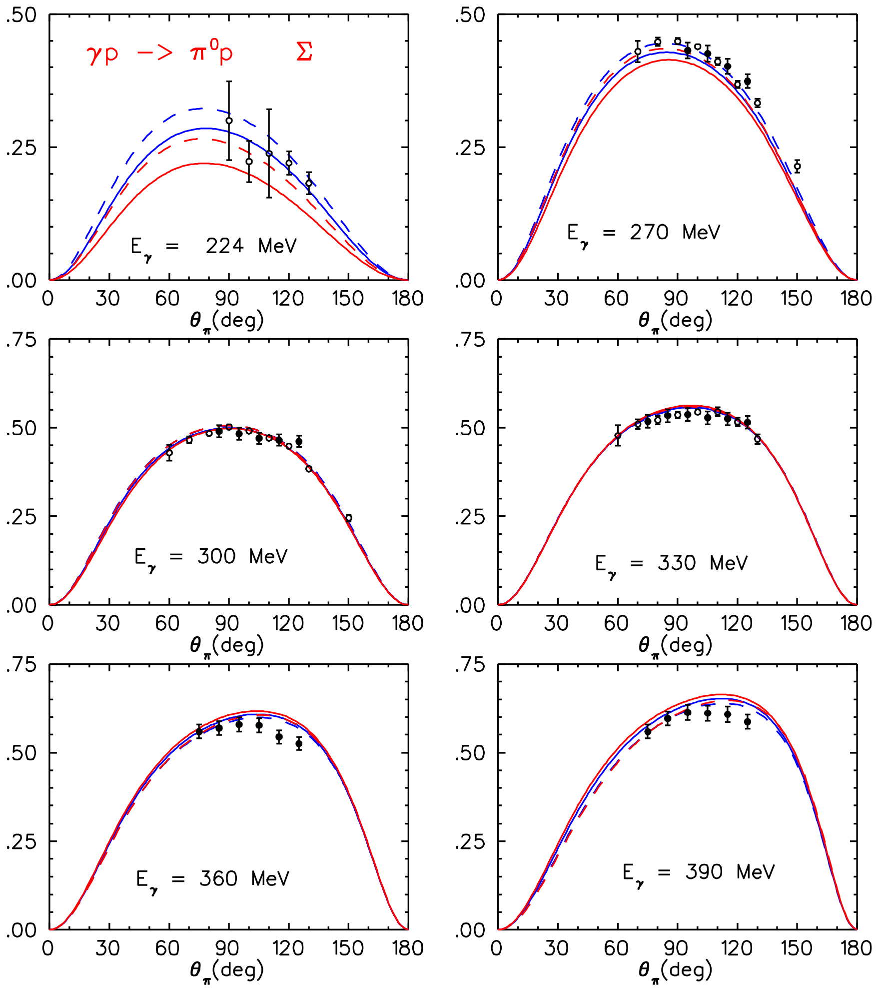

γp −> π⁰p Σ
E_γ = 224 MeV
E_γ = 270 MeV
E_γ = 300 MeV
E_γ = 330 MeV
E_γ = 360 MeV
E_γ = 390 MeV
θ_π(deg)

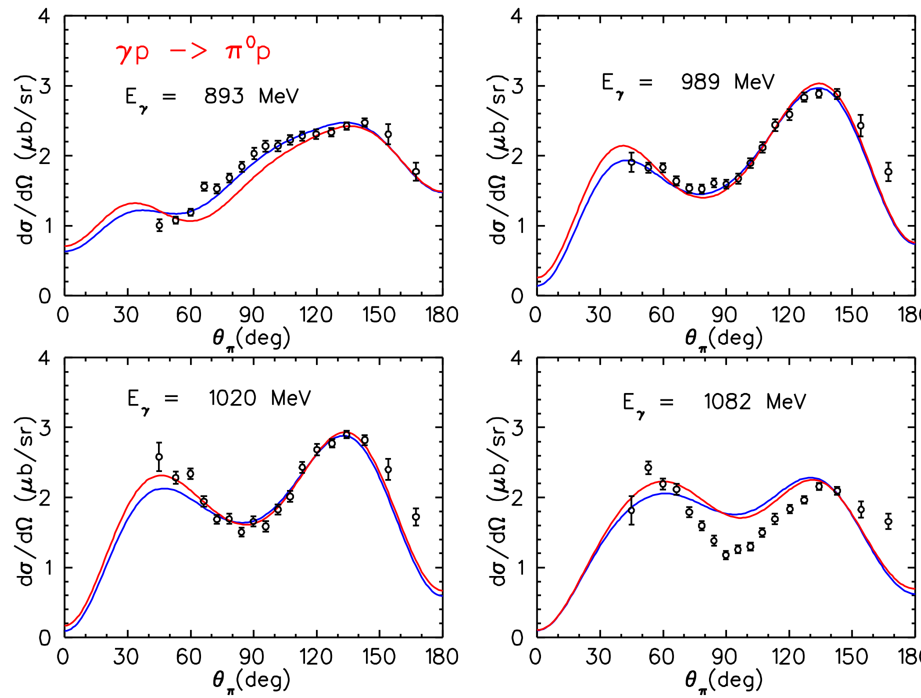

γp −> π⁰p
E_γ = 893 MeV
E_γ = 989 MeV
E_γ = 1020 MeV
E_γ = 1082 MeV
dσ/dΩ (μb/sr)
θ_π(deg)

results of our fits to the SAID s.e. partial waves

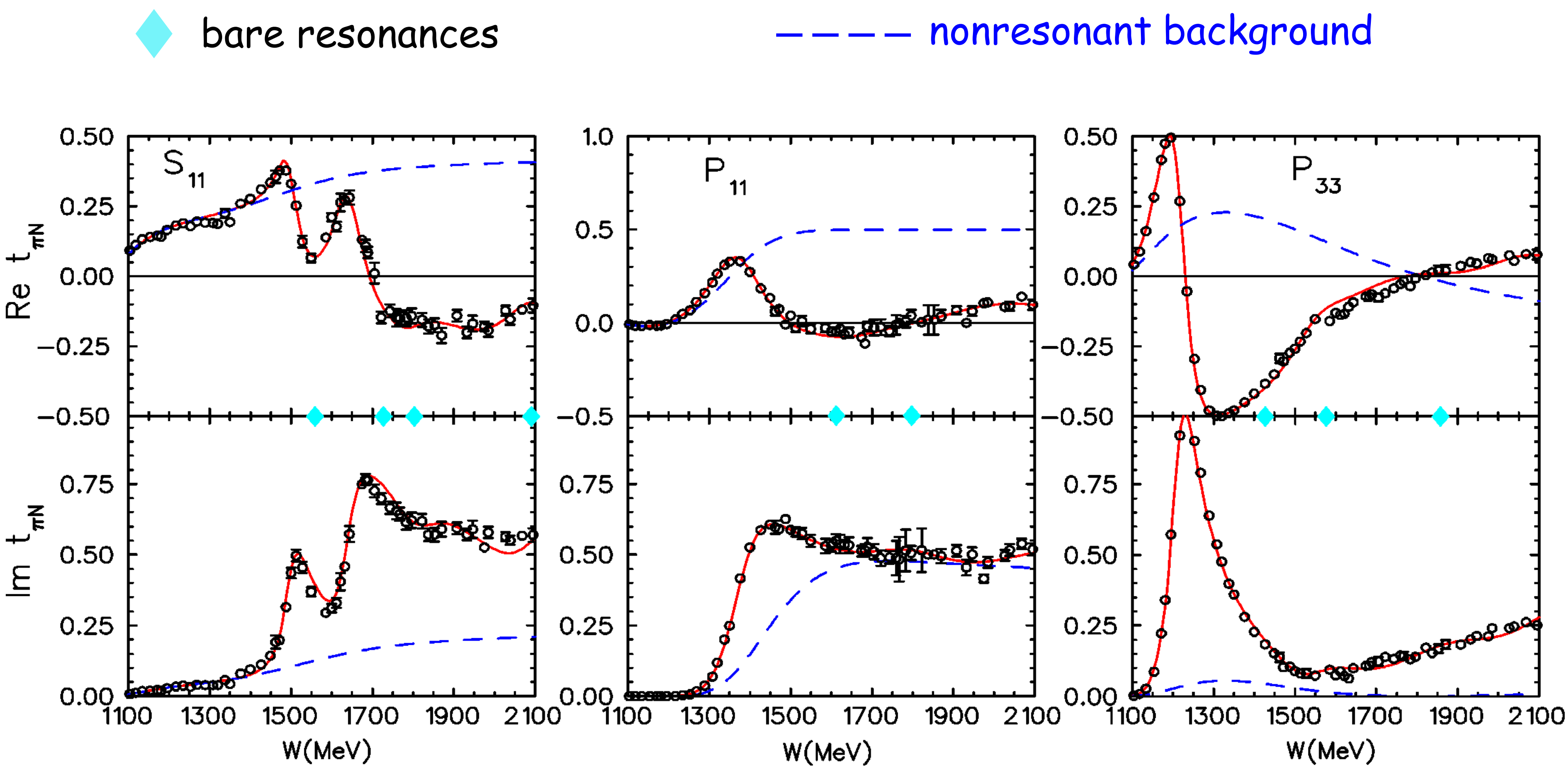

requires 4 resonances in S_{11}

single-energy pw analysis from SAID

Resonance masses, widths, and pole positions

bare and physical resonance masses, total widths, πN branching ratios and background phases for N* resonances (I=1/2)

bare phys

N^*	$M_R^{(0)}$	M_R	Γ_R	$\beta_R^{1\pi}$ (%)	ϕ_R (deg)
$P_{11}(1440)$ ****	1612	1418 1430±20	436 350±100	44 65±10	32
$D_{13}(1520)$ ****	1590	1520 1515±5	94 115±15	62 60±5	1.2
$S_{11}(1535)$ ****	1559	1520 1535±10	130 150±25	43 45±10	20
$S_{11}(1650)$ ****	1727	1678 1655±10	200 140±30	73 70±20	24
$D_{15}(1675)$ ****	1710	1670 1675±5	154 147±17	18 40±5	49
$F_{15}(1680)$ ****	1748	1687 1685±5	156 130±10	67 67±2	7.9
$D_{13}(1700)$ ***	1753	1747 1700±50	156 175±75	5 12±5	-1
$P_{11}(1710)$ ****	1798	1803 1710±30	508 150±100	32 12±8	40

our analysis
PDG
star * in red, upgraded in 2014

bare mass | physical mass

N^*	$M_R^{(0)}$	M_R	Γ_R	$\beta_R^{1\pi}$ (%)	ϕ_R (deg)
P_{13} (1720) ****	1725	1711 1725±25	278 225±75	13 11±3	0
P_{13} (1900) ****	1922	1861 ~1900	1000 ~250	18 ~5	-3.5
F_{15} (2000) **	1928	1926 2150±50	58 500±200	4 15±5	18
D_{13} (2080) **	1972	1946 1804±55	494 450±185	15 ~4	5
S_{11} (xxx)	1803	1878	508	41	-5
S_{11} (2090) *	2090	2124 2180±80	388 350±100	37 18±8	-18
P_{11} (2100) *	2196	2247 2125±75	1020 260±100	42 12±2	32
D_{13} (xxx)	2162	2152	292	14	7
P_{13} (xxx)	2220	2204	406	15	-4
D_{15} (2200) **	2300	2286 2180±80	532 400±100	16 10±3	8

our analysis
PDG

additional res. (S_{11} (xxx))
additional res. (D_{13} (xxx))
additional res. (P_{13} (xxx))

resonance parameters for Δ resonances (I=3/2)

bare mass | physical mass

N^*	$M_R^{(0)}$	M_R	Γ_R	$\beta_R^{1\pi}$ (%)	ϕ_R (deg)
$P_{33}(1232)$ ****	1425	1233 1232±1	132 117±3	100 100	12
$P_{33}(1600)$ ****	1575	1562 1600±100	216 320±100	6 17±7	-9
$S_{31}(1620)$ ****	1654	1616 1630±30	160 140±10	32 25±5	-41
$D_{33}(1700)$ ****	1690	1650 1710±40	260 300±100	15 15±5	-5
$P_{31}(1750)$ *	1765	1746 1744±36	554 300±120	4 8±3	-24
$S_{31}(1890)$ **	1796	1770 1885±25	430 280±60	8 22±7	-44
$F_{35}(1930)$ ****	1891	1854 1950±50	534 360±120	11 12±3	-12

our analysis
PDG

resonance parameters for Δ resonances (I=3/2)

bare mass | physical mass

our analysis
PDG

N^*	$M_R^{(0)}$	M_R	Γ_R	$\beta_R^{1\pi}$ (%)	ϕ_R (deg)
$P_{31}(1910)$ ****	1953	1937 1895±25	226 230±40	14 22±7	-21
$P_{33}(1920)$ ***	1856	1827 1935±35	834 240±60	12 12±7	3
$D_{35}(1930)$ ***	2100	2068 1950±50	426 360±140	15 10±5	-20
$D_{33}(1940)$ *	2100	2092 2057±110	310 460±320	6 18±12	-10
$F_{37}(1950)$ ****	1974	1916 1932±17	338 285±50	47 40±5	13
$F_{35}(2000)$ **	2277	2260 2200±125	356 400±125	11 16±5	-26
$P_{31}(xxx)$	2160	2100	492	35	-25
$S_{31}(2150)$ *	2118	1942 2150±100	416 200±100	70 8±2	-44

additional res.

Comparison with ANL-Osaka results

Features of ANL-Osaka vs. DMT

1. 8 coupled-channels

   (γN, πN, ηN, ~~σN, ρN, $\pi\Delta$~~, $K\Lambda$, $K\Sigma$)

2. different treatments in

   a. derivation of background potential

   b. prescription in maintaining gauge invariance

N* poles from ANL-Osaka DCC vs. DMT

$L_{2I\ 2J}$	PDG (MeV)	DMT	ANL-Osaka (MeV)
$S_{11}(1535)$	$(1490 \sim 1530) - (45 \sim 125)i$	$1449 - 34i$	$1482 - 98i$
(1650)	$(1640 \sim 1670) - (50 \sim 85)i$	$1642 - 49i$	$1656 - 85i$
$S_{31}(1620)$	$(1590 \sim 1610) - (60 \sim 70)i$	$1598 - 68i$	$1592 - 68i$
(1900)	$(1830 \sim 1910) - (65 \sim 115)i$	$1775 - 18i$	$1746 - 177i$
$P_{11}(1440)$	$(1350 \sim 1380) - (80 \sim 110)\mathrm{i}$	$1366 - 90i$	$1374 - 76i$
(1710)	$(1670 \sim 1770) - (40 \sim 190)i$	$1721 - 93i$	$1746 - 177i$
$P_{13}(1720)$	$(1660 \sim 1690) - (75 \sim 200)i$	$1683 - 120i$	$1703 - 70i$
(1900)	$(1870 \sim 1930) - (70 \sim 150)i$	$1846 - 90\mathrm{i}$	$1763 - 159i$
$P_{31}(1910)$	$(1830 \sim 1880) - (100 \sim 250)i$	$1896 - 65i$	$1854 - 184i$
$P_{33}(1232)$	$(1209 \sim 1211) - (49 \sim 51)i$	$1218 - 45i$	$1211 - 51i$
(1600)	$(1460 \sim 1560) - (100 \sim 175)i$	$1509 - 118\mathrm{i}$	$1734 - 176i$
$D_{13}(1520)$	$(1505 \sim 1515) - (52 \sim 60)i$	$1516 - 62i$	$1501 - 39i$
(1700)	$(1650 \sim 1750) - (50 \sim 150)i$	??	$1702 - 141i$
$D_{15}(1675)$	$(1655 \sim 1665) - (62 \sim 75)i$	$1657 - 66i$	$1650 - 75i$
$D_{33}(1700)$	$(1620 \sim 1680) - (80 \sim 150)i$	$1609 - 67i$	$1592 - 122i$
(1940)	$(1800 \sim 2000) - (70 \sim 130)i$	$2070 - 134i$	$1707 - 170i$
$F_{15}(1680)$	$(1665 \sim 1680) - (55 \sim 68)i$	$1663 - 58i$	$1665 - 49i$
$F_{35}(1905)$	$(1805 \sim 1835) - (132 \sim 150)i$	$1771 - 95i$	$1765 - 94i$
$F_{37}(1950)$	$(1870 \sim 1890) - (110 \sim 130)i$	$1860 - 100i$	$1872 - 103i$

Summary

- The DMT coupled-channel dynamical model gives excellent description of the pion scattering and pion photoproduction data from threshold up to $W \leqq 2$ GeV

  - Excellent agreement with π^0 threshold production data. Two-loop contributions small. DMT has become a benchmark/guide experiments and calculations for π^0 threshold production.

    cf. talk by Scherer

  - DMT predicts $\mu_{N\to\Delta}$ = 3.514 μ_N, $Q_{N\to\Delta}$ =-0.081 fm^2, and R_{EM}=-2.4%, all in close agreement with the experiments. $\Rightarrow$ dressed Δ is oblate

  - Bare Δ is almost spherical. The oblate deformation of the dressed Δ arises almost exclusively from pion cloud

- The resonance masses, width, and pole positions extracted with DMT agree, in general, with PDG and ANL-Osaka numbers, except we get 4 resonances not yet seen in PDG table:

  S11(1878), D13(2152), P13(2204), P31(2100)

DMT vs. ANL-Osaka

little dog vs. big tiger

but little could be effective

(小而美)

- Connection with LQCD

  cf. talks by and Edwards

END